

Numerical Calibration of Laboratory Results of 3D Printed Sandstone Analogues using Finite/Discrete Element Method (FDEM)

Dima Shamsedine

RWTH Aachen University, Department of Engineering Geology and Hydrogeology, Aachen, Germany

Pooya Hamdi

RWTH Aachen University, Department of Engineering Geology and Hydrogeology, Aachen, Germany

Florian Amann

RWTH Aachen University, Department of Engineering Geology and Hydrogeology, Aachen, Germany

Fraunhofer Research Institution for Energy Infrastructure and Geothermal Systems, IEG, Aachen, Germany

ABSTRACT: The study presents the first step of a research project that aims at investigating and modeling the geomechanical characteristics and failure mechanism of rock mass containing non-persistent rock joints using laboratory tests carried out on 3D printed sandstones. This paper focuses on modeling the behavior of intact sandstone analogues under compression and indirect tension tests using a 2D hybrid finite-discrete element method (FDEM) implemented in Irazu software. The advantage of FDEM approach is its ability to model the transition from continuum to discontinuum domain during intact rock fracturing. The models were calibrated against data sets of uniaxial/triaxial compression and Brazilian tests. Stress-Strain curves and failure mechanisms of models were compared to the experimental results, it was shown that the calibrated models could capture the strength and the brittle failure aspect of the sandstone analogues through crack initiation, propagation, and coalescence and are in good agreement with the laboratory results.

Keywords: FDEM, FEM-DEM, Calibration, Numerical Modelling, Uniaxial Compressive Strength (UCS), Triaxial Compressive Strength (TRX), Brazilian Test.

1 INTRODUCTION

The failure of a rock mass often occurs as a result of sliding along pre-existing discontinuities and defects and/or the breaking of intact rock bridges. This process can be described as a transition from a continuum to a discontinuum, as the failure begins with initiation and growth before merging into larger fractures. The Finite/Discrete Element Method (FDEM) pioneered by Munjiza (2004) is a hybrid method that combines both continuum and discontinuum approaches and has been widely used to model the behavior of brittle rocks, including interactions along pre-existing discontinuities and the formation of new fractures (Mahabadi and Lisjak 2014; Hamdi et al. 2015). FDEM also applies fracture mechanics principles to predict the initiation and development of fractures. When the failure criterion within the intact rock is met, a crack is initiated, and the model evolves from FEM into DEM.

The combination of FDEM with Discrete Fracture Network (DFN) can simulate the behavior of a rock mass with pre-existing fractures. DFN is a process of randomly generating a 3D representation of rock fractures that considers their primary characteristics including orientation, persistence, intensity, and spatial distribution to produce a realistic model of a rock mass (Hamdi et al. 2014, 2018). The rock mass consists of a complex interplay of two components: the intact rock and spatially distributed rock joints of various orientation and persistence. The first step towards modeling the behavior of a rock mass is the understanding of the behavior of the intact rock material. Upon that, the effect of different DFN characteristics on the overall behavior of the rock mass can then be examined distinctly. In this study, the FDEM method is used to model the behavior of 3D printed intact sandstone analogues using the Irazu software. Laboratory tests including uniaxial/triaxial compression and indirect tension tests were performed on the sandstone analogues prior the numerical modeling. The analogues exhibited a brittle behavior and had a uniaxial compressive strength UCS and tensile strength of 32.5 MPa and 5.5 MPa, respectively. The 2D models are then calibrated against the laboratory data sets and the results are discussed.

2 FEMDEM NUMERICAL MODELLING

The elastic deformation of intact rock is modeled using the linear elasticity theory with constant-strain triangular elements, taking into account the rock's Young's modulus E and Poisson's ratio ν , under the assumption of isotropic behavior. Interaction between discrete bodies is controlled by spatial hashing contact detection algorithm that detects contact between elements. If the method detects overlap between elements, repulsive and frictional forces are generated. This generation is controlled by the normal, tangential, and fracture penalty function (Mahabadi et al. 2016).

Fractures in the rock are simulated using a cohesive-zone approach with specialized four-node interface elements, known as crack elements, positioned along the edges of all triangular element pairs (Figure 1). The Mohr-Coulomb failure criterion is applied to the fractures generation as a reaction to the applied stresses, resulting in a change from continuous to discontinuous behavior (Mahabadi et al. 2012). Additionally, the Irazu software (<https://www.geomechanica.com/>) incorporates the concept of energy release rate (G), first introduced by Irwin (1957), to classify the three modes of fracturing processes of the modelled material: mode I for fracture opening through traction, mode II for fracture shearing, and mode III, also known as mixed mode, when both opening and shearing occur.

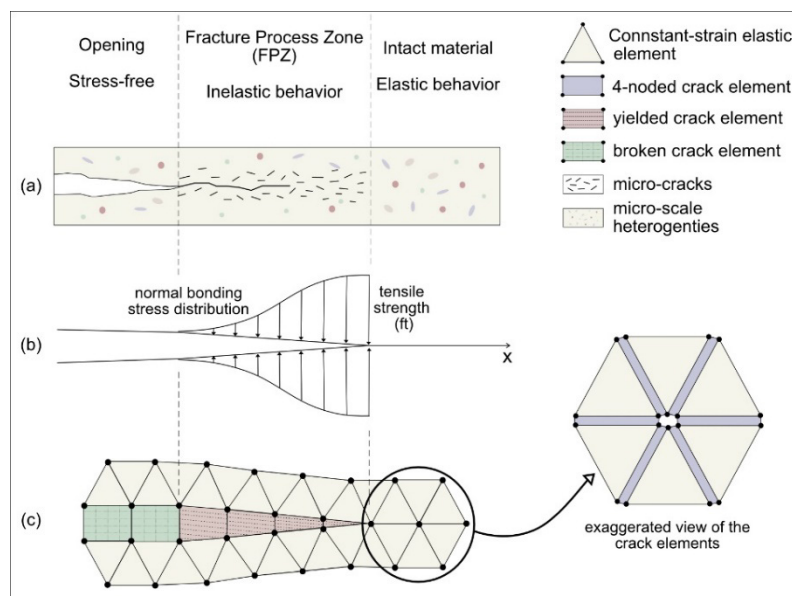


Figure 1. (a) Fracture process representation in brittle rocks, after Labuz et al. (1985); (b) normal bonding stress distribution along the fracturing zone, after Labuz et al. (1985); (c) numerical representation of the theoretical fracturing zone in the Irazu software, after Lisjak et al. (2014).

3 LABORATORY TEST DATA

The following numerical calibration is based on a data set obtained from the laboratory tests performed as a part of the research project, including uniaxial/triaxial compression, and indirect tension tests. The specimens were printed using Binder Jetting Printing (BJP) that uses silica-sand as core particles and furfuryl alcohol as the binder. Further details of the BJP method and the printing process can be found in Hamdi & Amann (2020). Table 1 represents the summary of results obtained from the laboratory tests on 3D printed synthetic specimens. The failure modes of the tested samples presented in Figure 2, will be used for comparison with the modelling results.

Table 1. Strength properties of the 3D printed synthetic sandstone obtained from the experimental campaign.

σ_t (MPa)	UCS (MPa)	Young's Modulus E (GPa)	Poisson's Ratio ν	Cohesion c (MPa)	Friction Angle ϕ (°)
4 - 6	31.5 - 33.5	2	0.05	11	15

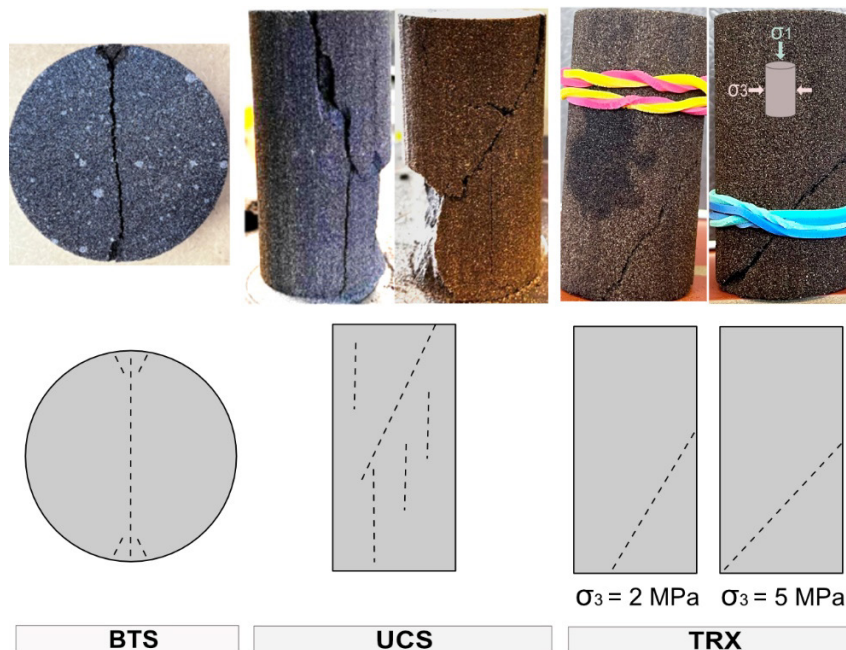


Figure 2. Examples of the failure mode of the 3D printed samples after Brazilian, UCS and TRX tests.

4 MODELS SIMULATIONS

The dimensions assigned to the numerical models are equal to the real dimensions of the 3D printed samples tested in the laboratory. The UCS cylinders are 100 mm in height and 50 mm in diameter, and Brazilian discs are 50 mm in diameter (Figure 3). The input files of the models are created and meshed (unstructured meshing) using the Gmesh software (<https://gmsh.info/>). The behavior of the specimen is assumed homogeneous and isotropic. The mesh size and compressive loading velocities are optimized to obtain accurate results and save computational time. The effect of the material properties of the compressing platens on the final results can be ignored since the same velocity is applied at each nodal point, making the platens behave as an infinitely rigid, non-destructible, material (Mahabadi et al. 2016). The hypothesis of plane stress and plane strain is proposed for UCS/TRX and Brazilian test simulations, respectively.

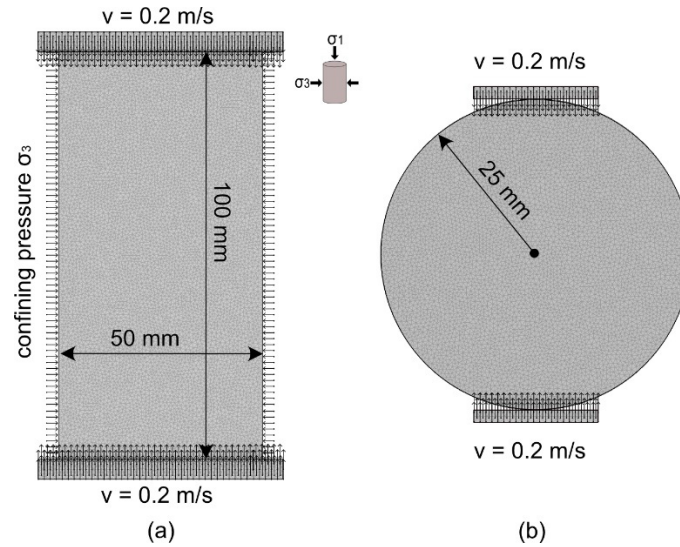


Figure 3. 2D numerical models of (a) UCS/TRX test simulations and (b) Brazilian test simulations; nominal mesh sizes are 1mm and 0.75mm for BTS and UCS models respectively.

The calibration procedure used in this study is adopted from the procedure presented in Tatone and Grasselli (2015). After creating the UCS and BTS geometries, the laboratory test results are primarily used as input parameters (UCS, E , ν , σ_t , c , and ϕ) for the models. The damping factor and the penalty values are then calibrated in a way to closely reach a model stiffness which best resembles the synthetic material stiffness. Secondly, both models are calibrated in order to obtain the desired cohesion, tensile strength and fracture energy input values that result in a good replication of the strengths and failure modes of the UCS and Brazilian test results. The last step of the models' calibration is against triaxial compression test, in which an appropriate friction angle value is chosen for the models to replicate the synthetic material's strength and failure mode during triaxial compression tests. The final set of the input parameters chosen to characterize the strength of the synthetic material and the loading platens is represented in Table 2.

Table 2. Input parameters of the synthetic sandstone and platen materials assigned to the 2D models in Irazu.

	Parameter	Platens	Sample
Elastic Parameters	Density ρ (kg/m ³)	7000	1600
	Young's Modulus E (GPa)	200	2
	Poisson's Ratio ν	0.3	0.05
	Friction Coefficient	0	0.2
Strength Parameters	Cohesion c (MPa)	200	11
	Tensile Strength σ_t (MPa)	200	5.5
	Mode I Fracture Energy ($\mu\text{N}/\text{mm}$)	3.3E+05	1E+05
	Mode II Fracture Energy ($\mu\text{N}/\text{mm}$)	3.3E+06	9E+05

5 NUMERICAL RESULTS

The stress-strain plots obtained for simulated UCS and TRX models are shown in Figure 4a. The calculated UCS and Young's Modulus (E) for the models are 30 MPa and 1.9 GPa, respectively, which are in good agreement with the strength value ranges obtained from laboratory tests. Stress strain analysis on laboratory triaxial tests showed an increase in the strength of the specimen upon increasing the applied confining pressure, and the post peak behavior changes gradually from brittle to ductile by increasing the confining pressure (i.e. confining pressure > 5 MPa). The strength values obtained from the calibrated model agree well with obtained triaxial strengths. It is noted that no

effort is made to replicate the transition from brittle to ductile post peak behavior at a higher confining pressure as the objective of the project is to study the behavior of rock mass in the brittle region. Therefore, numerical model results are only compared to data points obtained from TRX samples tested under confining pressures $\leq 5 \text{ MPa}$ (i.e. failed in a brittle manner). The indirect tensile strength of the Brazilian disc model recorded 3.8MPa, which is an underestimation (27% difference from laboratory results) of the actual synthetic material strength (5.5MPa). The underestimation can be attributed to the fact that the σ_t/UCS ratio obtained from the laboratory tests is relatively high compared to the average range of ratios for natural brittle rocks $1/20 - 1/10$.

The failure mode of the UCS model shows a combination of axial splitting and shear failure (distinguished from the fracture color), indicating a good resemblance of the experimental failure mode shown in Figure 2. Failure of the Brazilian disc model is valid, starting from the center of the disc and propagating towards the contact points with loading platens Figure 5. Figure 4b shows the best-fitted Mohr-Coulomb envelope to the laboratory results and the calibrated models. Despite some minor discrepancy, the numerical results show a good agreement with experimental test results. The obtained fracture pattern of the TRX models shows a shear domination which is also in agreement with laboratory results, indicating a transition from axial splitting with dominant tensile at low to no confining pressure to shear dominant fracturing at a higher confining pressure.

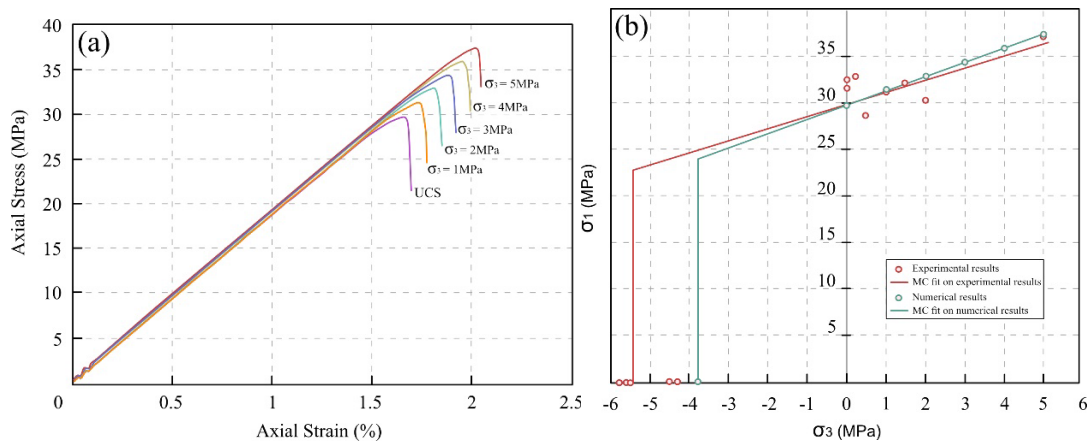


Figure 4. (a) Stress-strain curves obtained from modeled UCS and TRX; (b) Comparison of the Mohr coulomb curve fits to the numerical and experimental results.

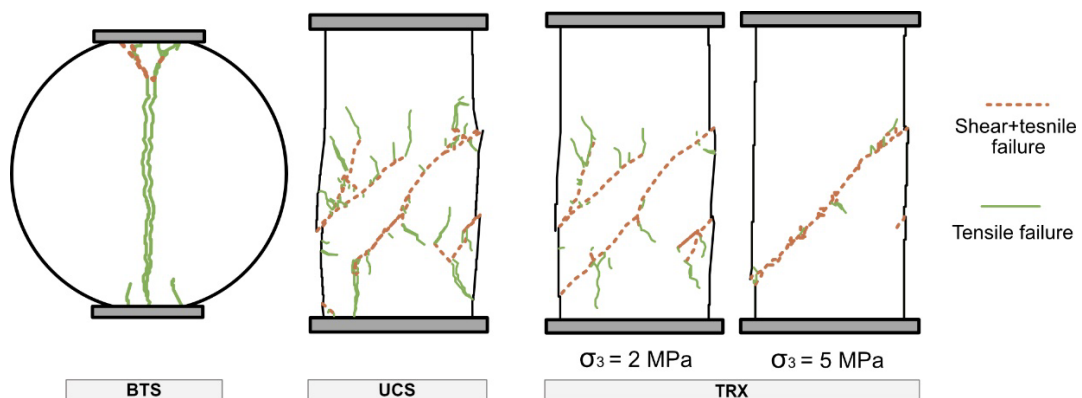


Figure 5. Failure modes of the 2D models under Brazilian test, uniaxial test, and triaxial test simulations.

6 DISCUSSION AND CONCLUSION

This paper presents the results of 2D numerical models calibrated on laboratory tests data sets done on synthetic rock analogues. The purpose was to replicate the strength and the behavior of the intact

rock analogues under different stress regimes, using finite discrete element method implemented in the Irazu software. The UCS model failed at 30MPa, and exhibited a combination of extensional, and shear fractures, agreeing well with the laboratory UCS results. The tensile strength of the Brazilian disc model (4MPa) showed an underestimation of the experimental tensile strength (27% error). The model showed a gradual increase in its strength upon applying higher confinement pressures during TRX simulations and a change of the failure mode from extensional fracturing domination at no to low confinement, to shearing domination at higher confinement (5MPa). Mohr-Coulomb envelopes fitted on numerical and experimental results showed an acceptable resemblance, indicating that the modelled material can successfully replicate the behavior of the synthetic rock analogues.

REFERENCES

- Hamdi P, Amann F (2020) Evaluating the Influence of Rock Bridge Characteristics: Rock Bridge Percentage and Spatial Location, on the Strength of a Synthetic Rock Mass – Experimental Approach. *OnePetro*
- Hamdi P, Stead D, Elmo D (2014) Characterizing the influence of micro-heterogeneity on the strength and fracture of rock using an FDEM- μ DFN approach. In: *ISRM European Rock Mechanics Symposium, EUROCK*. Vigo, Spain, p 6
- Hamdi P, Stead D, Elmo D (2015) Characterizing the influence of stress-induced microcracks on the laboratory strength and fracture development in brittle rocks using a finite-discrete element method-micro discrete fracture network FDEM- μ DFN approach. *J Rock Mech Geotech Eng* 7:609–625. <https://doi.org/10.1016/j.jrmge.2015.07.005>
- Hamdi P, Stead D, Elmo D, Töyrä J (2018) Use of an integrated finite/discrete element method-discrete fracture network approach to characterize surface subsidence associated with sub-level caving. *Int J Rock Mech Min Sci* 103:55–67. <https://doi.org/10.1016/j.ijrmms.2018.01.021>
- Irwin GR (1957) Analysis of Stresses and Strains Near the End of a Crack Traversing a Plate. *J Appl Mech* 24:361–364. <https://doi.org/10.1115/1.4011547>
- Labuz JF, Shah SP, Dowding CH (1985) Experimental analysis of crack propagation in granite. *Int J Rock Mech Min Sci Geomech Abstr* 22:85–98. [https://doi.org/10.1016/0148-9062\(85\)92330-7](https://doi.org/10.1016/0148-9062(85)92330-7)
- Lisjak A, Tatone BSA, Grasselli G, Vietor T (2014) Numerical Modelling of the Anisotropic Mechanical Behaviour of Opalinus Clay at the Laboratory-Scale Using FEM/DEM. *Rock Mech Rock Eng* 47:187–206. <https://doi.org/10.1007/s00603-012-0354-7>
- Mahabadi O, Lisjak A (2014) Application of FEMDEM to analyze fractured rock masses. <https://doi.org/10.13140/2.1.4463.9687>
- Mahabadi O, Lisjak A, Munjiza A, Grasselli G (2012) Y-Geo: New Combined Finite-Discrete Element Numerical Code for Geomechanical Applications. *Int J Geomech* 12:676–688. [https://doi.org/10.1061/\(ASCE\)GM.1943-5622.0000216](https://doi.org/10.1061/(ASCE)GM.1943-5622.0000216)
- Mahabadi OK, Lisjak A, He L, et al (2016) Development of a New Fully-Parallel Finite-Discrete Element Code: Irazu. *OnePetro*
- Munjiza A (2004) *The Combined Finite-Discrete Element Method*, 1st edn. Wiley
- Tatone BSA, Grasselli G (2015) A calibration procedure for two-dimensional laboratory-scale hybrid finite-discrete element simulations. *Int J Rock Mech Min Sci* 75:56–72. <https://doi.org/10.1016/j.ijrmms.2015.01.011>